



## Thermal Performance of a Mechanical Thermostat for Charging an Energy Storage System

Swaleh Tusiime<sup>1,\*</sup>, Karidewa Nyeinga<sup>1</sup>, Denis Okello<sup>1</sup> and Ole J. Nydal<sup>2</sup>

<sup>1</sup>Department of Physics, Makerere University, P.O. Box 7062 Kampala, Uganda.

<sup>2</sup>Department of Energy and process Engineering, Norwegian University of Science & Technology (NTNU), P.O. Box 7491, Trondheim, Norway.

\* Corresponding author: [tmswlh2@gmail.com](mailto:tmswlh2@gmail.com); [swaleh.tusiime@mak.ac.ug](mailto:swaleh.tusiime@mak.ac.ug)

Received 1 Mar 2023, Revised 26 May 2023, Accepted 1 June 2023 Published June 2023

DOI: <https://dx.doi.org/10.4314/tjs.v49i2.1>

### Abstract

Thermal energy storage (TES) systems enhance the use of solar energy for cooking by matching the energy demand to its supply. Useful energy is extracted from TES systems that are thermally stratified and this is enhanced when charged at an averagely constant-temperature. This paper presents an experimental analysis of a mechanical-thermostat used to control the charging of an oil based TES system. The thermostat consisted of a slider-valve, an expansion-system acting both as a thermal-sensor and actuator, and an adjusting-knob for setting the charging temperature. Oil from a cold-oil reservoir flows by gravity into a heating-chamber when a manual valve is opened. In the heating-chamber, the oil is heated causing the oil to expand triggering the opening of the slider-valve at a preset temperature. This allows the hot-oil to flow into the TES system at the set temperature. The thermostat was demonstrated for charging a TES system at preset temperatures of 116 °C, 150 °C, 200 °C and 230 °C. The volume of hot-oil delivered into a TES tank decreased with increasing charging temperature. The observed temperature variations were minimized by reducing the oil flow-rate using a valve hence achieving a fairly stable charging temperature.

**Keywords:** Mechanical thermostat; Charging temperature; Thermal energy storage system, Solar energy, Cooking.

### Introduction

The use of wood fuel for cooking purposes among others has led to high deforestation rates, inhaling smoke particles from burning wood and increasing the concentrations of greenhouse gases in the earth's atmosphere (Schwarzer and da Silva 2008, Kitutu and Diisi 2014). This calls for the need to use alternative renewable energy resources, such as geothermal energy, hydro-power, wind, and solar energy. Solar energy has the potential to solve this cooking energy problem when harnessed with appropriate technologies. For cooking purposes, it is preferred to directly harness the thermal form of solar energy (Herrmann and Kearney

2002, Cuce and Cuce 2013). It is also desired to use solar cookers with thermal energy storage (TES) system which attempts to regulate the mismatch between energy demand and energy supply due to the intermittent nature of solar energy (Okello et al. 2016, Lugolole et al. 2018, Kajumba et al. 2020).

Improving thermal stratification of a TES system improves the efficiency and quality of heat extraction from it (Sharp and Loehrke 1979, Haller et al. 2009). The different expressions of thermal stratification show that, thermal stratification in an oil-based TES system can be improved when charged at a fairly constant temperature (Fernandez-

Seara et al. 2007). Hence, the need to control the temperature of the hot oil flowing into the TES system using a thermostat. More so, the challenge of delivering the oil into the TES tank at any temperature means that the cold oil from the reservoir tank has to be re-circulated for a long time before it can attain high temperatures suitable for cooking (Mawire et al. 2014), hence cooking cannot be started immediately. Otherwise if the heated oil is delivered into the TES tank at the suitable temperature, cooking could be started immediately or after a short time once charging has started. However, to achieve this, a suitable thermostat which can operate at the required temperatures is desired.

Previous attempts to charge an oil based TES system at a relatively constant temperature showed that the temperature of oil delivered to the TES system varied within a range of 50 °C while charging at 200 °C (Hansen and Boggsnes 2018). The charging temperature of 200 °C was preferred, based on previous experiments (Gallagher 2011, Okello et al. 2022). Hence the need for a suitable thermostat that could further reduce the variations in the charging temperature.

Mechanically triggered thermostats are preferred over electronic/electrical thermostats in this case due to the high temperatures involved (200–350 °C). The available mechanical thermostats on the market are not purely mechanical but a combination of both mechanical and electronic/electric components and they operate at low temperatures (e.g. 100 °C). The mechanism of mechanical thermostats is based on the expansion of the heated fluid which results into the switching on or off of the actuator and hence regulating the fluid flow. This expansion mechanism can be used to open a flow pipe at a preset temperature analogous to solenoid valves in washing machines. The available solenoid valves cannot be used because they contain plastic components that cannot withstand the high temperatures involved. Therefore, there is need to develop a purely mechanical

thermostat suitable for charging oil based TES systems at a fairly constant high temperature.

This study was aimed at constructing and testing the performance of a mechanical thermostat that regulates the charging temperatures of oil-based TES systems for cooking purposes. The system was demonstrated in charging a TES system at various set temperatures. The objective of the study was to conduct a thermal performance test of the mechanical thermostat that regulates the charging process for an oil based TES system.

## Materials and Methods

### Design and construction of the components of the mechanical thermostat

Figure 1 shows the schematic diagram of the mechanical thermostat. It consists of: the heating chamber where the oil gets heated, the slider-valve for opening and closing for the oil to flow into the TES system, the expansion system for controlling the slider-valve by the expansion and contraction of oil due to temperature changes and the adjusting knob for setting the charging temperature. Each component was constructed, and later assembled together as described in the following sections.

### The heating chamber

The heating chamber was a cuboidal container open at the top to the atmosphere, with a heater 800W 220 V AC fixed at the bottom and part of the copper coil as shown in Figure 1. It was constructed by welding mild steel sheet to a cuboid open at the top with a height of 0.5 m, width of 0.08 m, and length of 0.04 m. Two holes of diameter 0.013 m each, were drilled 0.3 m apart along a vertical line on one side of the heating chamber. The hole at the bottom was used as inlet for cold oil into the heating chamber, while the hole at the top as outlet for hot oil into the storage tank through the slider-valve.

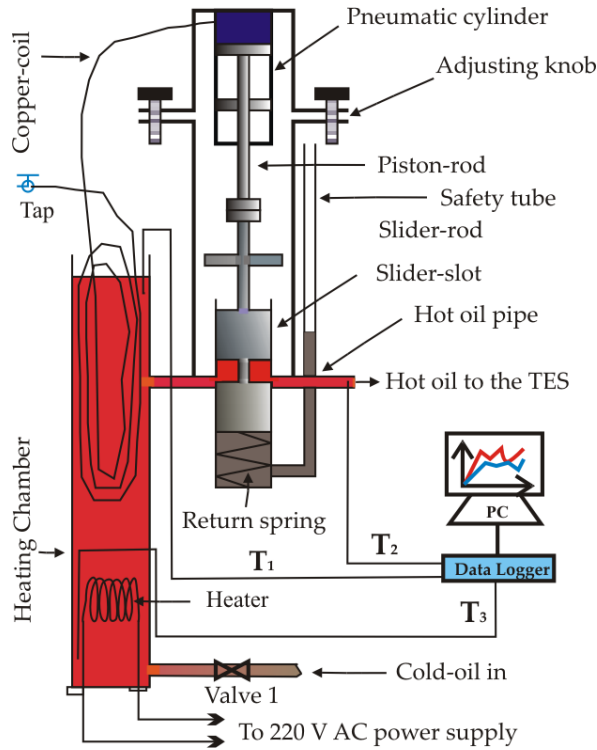


**Figure 1:** Schematic diagram showing the components of the mechanical thermostat.  $T_1$ ,  $T_2$  and  $T_3$  are temperatures of the oil: at the top of the heating chamber, from the slider-valve to the TES system; and at the bottom of the heating chamber, respectively.

### The slider-valve

The slider-valve was composed of a mild steel rod (slider-rod) of diameter 0.02 m that moves freely inside a pipe (slider-slot) as shown in Figure 2. The slider-slot had two holes on opposite sides acting as oil inlet and outlet points. Oil from the heating chamber only passes through the slider-valve into the TES system when the slider-valve is opened. A return spring with a force constant of  $2.0 \times 10^3 \text{ Nm}^{-1}$  was fixed at the bottom of the slider-valve. This return spring helps to ensure that the slider-valve is always closed.

The force constant of the return spring was determined by hanging known masses on the spring and measuring its extension. A small safety pipe open to the atmosphere was welded at the bottom of the slider slot to avoid compressing oil. The slider-rod is moved by the piston-rod to open the slider-valve when the oil expansion exceeds a certain limit. This limit is determined by the position of the oil inlet and outlet pipes relative to the oil-flow provisions in the slider-rod.

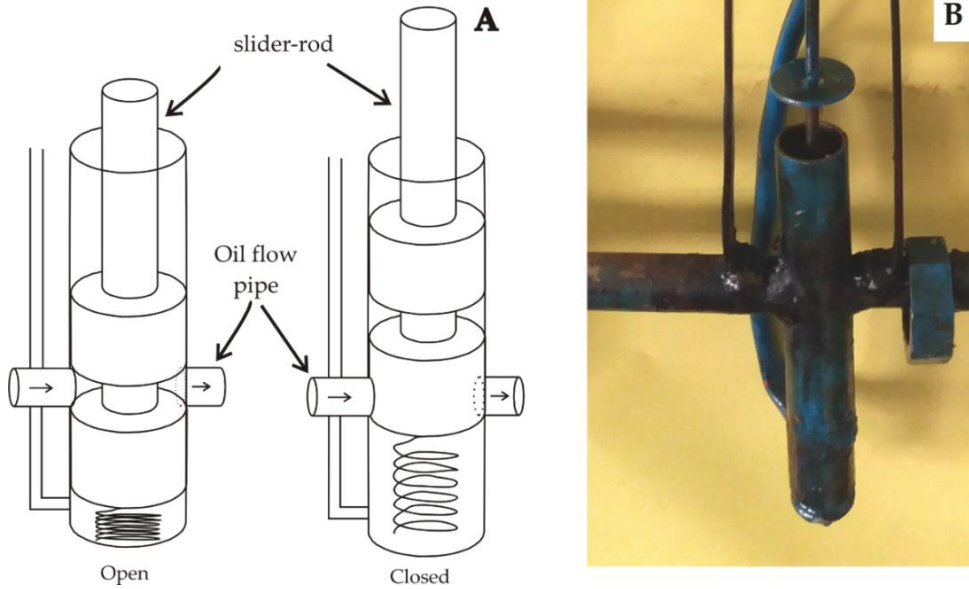


**Figure 2:** (A) Schematic diagrams illustrating the opening and closing of the slider-valve; (B) Photograph of the assembled slider-valve.

### The expansion system

The expansion system was composed of a copper coil welded to the pneumatic cylinder at one end, with a closing tap at the other end as shown in Figure 3. It was filled with oil ensuring that the system is air-free. A section of the copper coil was coiled 18 turns, each of length 0.2 m so that it could fit into the heating chamber. The piston-rod of the

pneumatic cylinder was attached to the slider-rod so that they move together. The pneumatic cylinder had a stroke length of 0.05 m and diameter of 0.025 m. The copper coil had a length of 4.0 m and internal diameter of 0.071 m. The expansion system was filled with Shell thermia B oil whose material properties are known (BPS 2005).



**Figure 3:** Photograph of the expansion system consisting of a copper coil and pneumatic cylinder.

### The Adjusting Knob

The adjusting knob was a set of bolts and nuts designed to increase or decrease the distance between the slider-valve and the pneumatic cylinder as shown in Figure 1 and Figure 4. By increasing or decreasing this distance, the charging temperature at which the slider-valve opens for hot oil to flow to the TES system would be lowered or increased, respectively.

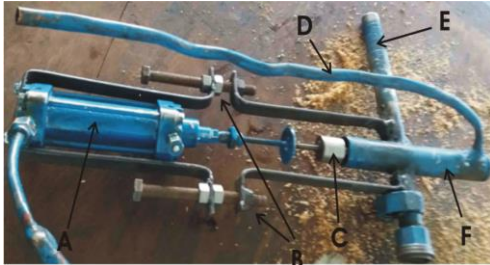


**Figure 4:** Photograph showing the adjusting knob and how it was attached to other components. The labels in the photograph represent the: (A) pneumatic cylinder, (B) adjusting knobs, (C) slider-rod, (D) safety tube, (E) hot oil pipe, and (F) slider-slot.

Other equipment used in this experiment included: k-type thermocouples and a Pico data logger (USB-TC-08) which were used to measure and record the temperatures-time series for the selected points, respectively. The cold oil reservoir tank for storing cold oil was fabricated locally from a 0.001 m mild steel sheet into a cylinder with a diameter and height of 0.38 m and 0.36 m, respectively. A steel cylinder with height and diameter equal to 0.3 m was used as a hot oil storage tank.

### Assembling the thermostat components

The cold oil reservoir was connected to the bottom of the heating chamber using a pipe of internal diameter 0.013 m. The coiled part of the copper coil was positioned above the heater in the heating chamber. Only about three-quarters of the coiled part of the copper coil could fit in the top part of the heating chamber since the heater had occupied the bottom part. The expansion system and the slider-valve were put together according to the schematic in Figure 1. The oil outlet from the slider-valve was directed into the storage

tank. Thermocouples were positioned to measure temperatures of oil at the top ( $T_1$ ) of the heating chamber, at the slider-valve outlet ( $T_2$ ), and at the bottom ( $T_3$ ) of the heating chamber as shown in Figure 1.

### Experimental set-up and procedure

The different components of the mechanical thermostat were assembled together as shown in the experimental setup in Figure 5. The cold oil reservoir was filled with 16 litres of cold oil (Shell thermia B). The valve was opened to let cold oil from the reservoir to flow into the heating chamber due to the pressure difference  $\Delta P$  until the oil levels in the two were the same. The flow of oil due to this pressure difference is governed by the Darcy-Weishbach Equation (1) (Brown 2002).

$$\frac{\Delta P}{L} = \lambda \rho \frac{v_l^2}{2 D} \quad (1)$$

where  $L$  is length traversed by the flowing liquid from the cold oil reservoir to the TES system,  $v_l$  is velocity of the oil,  $\rho$  is density of the oil,  $D$  is average diameter of the pipe through which the oil flows and  $\lambda$  is the Darcy friction factor.

The heater, connected to mains grid, was used to heat the oil in the heating chamber according to Equation (2) (Mawire et al. 2010):

$$\dot{Q} = \rho c v (T_1 - T_3) \quad (2)$$

where  $c$  is specific heat capacity of the oil,  $v$  is the volumetric flow rate,  $T_1$  is the average temperature of oil leaving the heating chamber,  $T_3$  is the temperature of oil entering the heating chamber and  $\dot{Q}$  is the power rating of the heater. The heated oil rises to the top and in-turn heats the oil in the copper coil which expands forcing the slider-valve to open. The expansion of the oil, i.e., the change in volume,  $\Delta V$  due to a temperature change,  $\Delta T$ , is given by Equation (3) (Sjogren and Steen 2018).

$$\frac{\Delta V}{V} = \alpha \Delta T, \quad (3)$$

where  $\alpha$  is thermal expansion coefficient.

The opening of the slider valve allows hot oil to flow into the TES tank at the preset charging temperature. However, this creates a pressure difference  $\Delta P$  again between the heating chamber and the cold oil reservoir as a result of the flow of hot oil into the heat storage tank. This pressure difference leads to the flow of more cold oil from the reservoir into the heating chamber; thereby lowering the average oil temperature in the heating chamber and in the copper coil. The cooling of oil in the copper-coil leads to oil contraction in the expansion system hence the closure of the slider-valve with the help of the return spring. This process of opening and closing of the slide-valve is repeated as heating continues. Hence, hot oil at the preset temperature would flow into the storage tank.



**Figure 5:** Photograph showing the experimental setup for testing the mechanical thermostat. The labelled components include the: (A) heating chamber, (B) cold oil reservoir, (C) slider-valve and (D) temperature data logger.

### Testing the expansion system

The system was tested to ensure that the expansion system was able to deliver hot oil into the storage tank at a preset charging temperature of about 200 °C. More so, some

oils get oxidized when kept for longer periods leading to a change in their properties (Crapiste et al. 1999). The heater was switched on to heat the oil in the heating chamber to a temperature of about 200 °C, switched off and let to cool. During the heating and cooling process, the displacement of the piston-rod and the oil temperature were measured and recorded using a Vernier caliper and thermocouples, respectively. The displacement of the piston rod at 200 °C was used to determine the position on the slider-slot where to drill the hole for the hot oil to flow into the TES system.

During the cooling process, the height of oil level from the bottom of the heating chamber was measured at the oil temperature of 200 °C and at ambient temperature of 25 °C, then used to re-estimate the coefficient of volume expansion. The thermal expansion coefficient was determined as the ratio of the measured relative change in volume to the corresponding temperature change. The uncertainty,  $\delta\alpha$  in the re-estimated thermal expansion coefficient was determined using the expression in Equation (4) (Hand 2011)

$$\delta\alpha = \alpha \sqrt{\left(\frac{\delta\Delta V}{\Delta V}\right)^2 + \left(\frac{\delta V}{V}\right)^2 + \left(\frac{\delta\Delta T}{\Delta T}\right)^2}, \quad (4)$$

where  $\delta V$ ,  $\delta\Delta V$  and  $\delta\Delta T$  are the uncertainties in; volume of oil, change in the oil volume and in the temperature change. Since the whole copper coil is not heated uniformly, then an equivalent oil volume that could be heated uniformly to produce the same effect had to be estimated and is vital in repeating the experiment with an improved expansion system. The error expression in Equation (5) for the equivalent oil volume  $V$  was extracted from Equation (3) using the standard error analysis approach (Hand 2011).

$$\delta V = V \sqrt{\left(\frac{\delta\Delta V}{\Delta V}\right)^2 + \left(\frac{\delta\alpha}{\alpha}\right)^2 + \left(\frac{\delta\Delta T}{\Delta T}\right)^2}, \quad (5)$$

### Setting the thermostat to a constant charging temperature

Equation (2) shows that the charging temperature,  $T$ , is affected by the flow rate,  $v$ , at a constant heating rate  $\dot{Q}$ . Of the factors provided by Equation (1) affecting the flow rate, i.e., the average pipe diameter is easier to adjust using a valve along the oil flow path. The effect of the variations in the charging temperature when the valve was half-way and quarter-way opened were demonstrated.

## Results and Discussion

### Testing the performance of the expansion system

Figure 6 shows the displacements of the piston rod at various temperatures during the heating and cooling processes while testing the expansion system. Figure 6 shows that at

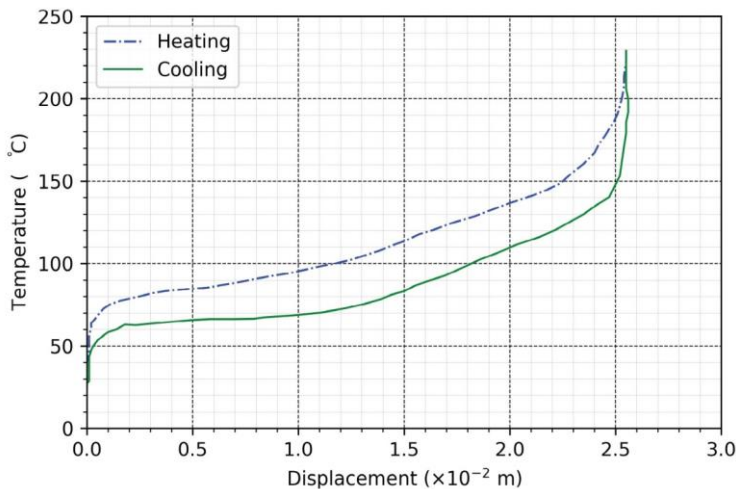


**Figure 6:** Variations of the measured temperatures and displacements due to thermal expansion of shell thermia B oil in the expansion system during the heating and cooling processes.

### Charging temperature profiles

Figure 7 shows the temperature profile and volume of the hot oil collected at the pre-set charging temperature of 116 °C, 150 °C and 230 °C with the valve fully open. The charging temperature is the temperature at which the slider-valve was expected to open for hot oil to flow into the TES tank. At all charging temperatures, the oil temperature at the top of the heating chamber,  $T_1$ , is

low temperatures (below 50 °C), there are negligible displacements due to minimal oil expansion and stickiness of the oil at low temperatures. Above 50 °C, as the temperature increases, the displacement also increases due to the expansion of oil in the expansion system. The oil expands linearly with temperature according to Equation (3), however, at high temperatures (above 150 °C), an exponential decrease in expansion is observed due to compressing the return spring. During cooling, the same trend is observed though the same path could not be traced due to thermal loss to the ambient and friction in the pneumatic cylinder and slider-valve. The maximum displacement of the piston-rod was 0.026 m at 200 °C. It is at this point on the slider-slot where a hole was drilled for the opening that lets oil flow to the slider-valve from the heating chamber.

observed to increase from ambient to the set charging temperature, thereafter it starts to oscillate.

During the three charging temperatures, the heat supplied is used to raise the oil temperature in the heating chamber to the preset charging temperature, when the slider-valve opens. The oil in the expansion system expands during the heating process pushing the piston-rod to open the slider-valve. When

the slider-valve opens, the hot oil flows into the TES system creating a pressure difference that leads to the flow of cold oil into the heating chamber according to Equation (1). The flow of cold oil into the heating chamber leads to the cooling and contraction of oil in the copper coil causing the slider-valve to close with the help of the return spring. This process of opening and closing the slider-valve repeats itself resulting into the variations in flow rate, temperatures  $T_1$  and  $T_2$  and the stepwise increase in the volume of hot oil collected. The difference between the temperatures  $T_1$  and  $T_2$  is due to thermal losses between the slider-valve and the heating chamber.

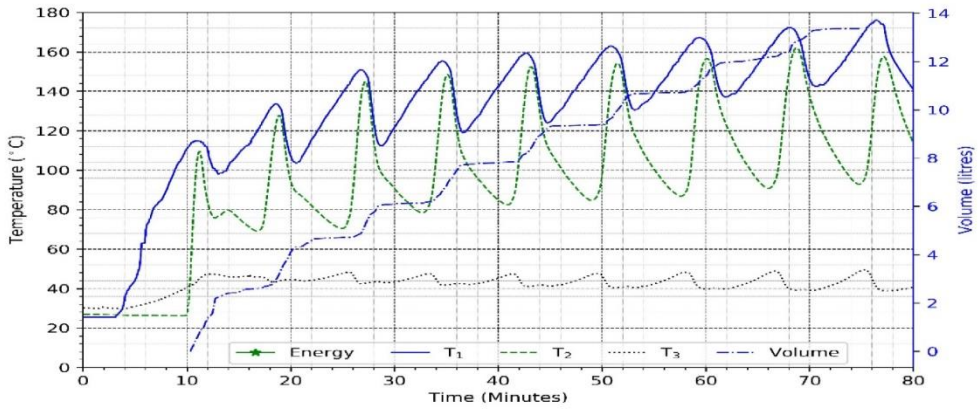
The average of the oscillations in temperature  $T_1$ , increased with time. This was attributed to the fact that, the copper coil (part of expansion system) was not fully immersed into oil in the heating chamber making its thermal losses vary with temperature of surrounding air. The inlet oil temperature  $T_3$  is at ambient at the inlet point but gets heated by conduction from the top hot oil up to about 40 °C depending on the temperature of the top hot oil.

The observed variations in the charging temperatures in Figures 7 are considered to be oscillations due to the automatic opening and closing of the slider-valve. Analogous to classical oscillatory systems, we had an under damped expansion system. It is desired to have a critically damped expansion system.

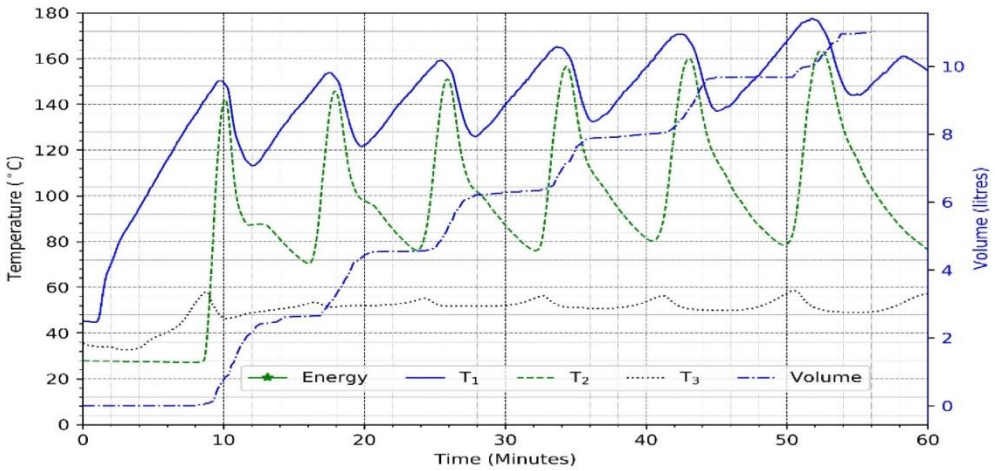
In general, oscillations are due to the mismatch between the responses between two systems or system components (Kilian 2001). The responses in our case of this mechanical thermostat are from the cold oil reservoir and the expansion system. For the expansion system, heating oil leads to the opening of the slider-valve and cooling the oil leads to its closure. The slider-valve opens due to the expansion of oil in any part of the expansion system and its closure is due to the contraction of this oil with the help of the return spring.

The oscillations in this thermostat are due to the slow response of the expansion system compared to the faster flow response of the cold oil reservoir when the slider-valve opens. In this experiment, we could not measure the response times of these systems. But, the response of the cold oil reservoir depends on the pressure head in it while for the expansion system it depends on; the coefficient of volume expansion of the oil in it, the friction in the pneumatic cylinder and in the slider-valve. Equation (1) gives the factors affecting this oil flow and one of them could be used to control this flow. Equation (2) shows that the volumetric flow rate affects the charging temperature  $T_1$  and could be used to attain the desired thermal regulation. In our case, we only had access to controlling or varying the average diameter of the flow pipe by partially opening the valve so as to attain a fairly constant charging temperature.

(a) Charging at 116 °C



(b) Charging at 150 °C



(c) Charging at 230 °C

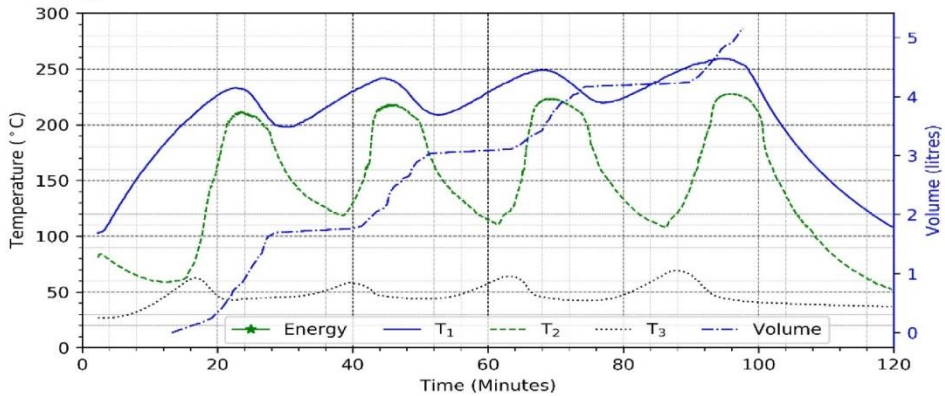


**Figure 7:** Temperature profiles of oil at the top of the heating chamber (T<sub>1</sub>), at the slider outlet (T<sub>2</sub>), at the bottom of the heating chamber (T<sub>3</sub>), and volume of hot oil collected in the heat tank while charging at a pre-set temperatures of: (a) 116 °C, (b) 150 °C and (c) 230 °C.

### Achieving a fairly constant charging temperature

The observed oscillations in the charging temperature profiles in Figures 7 were obtained with the valve fully opened. Figure 8 shows temperature profiles obtained when the valve was half-way opened at a preset charging temperature of 200 °C.

Figure 8 shows that the oil temperature  $T_1$  in the heating chamber increases up to about 125 °C in 2 minutes and the slider-valve opened. The temperature  $T_1$  dropped slightly as temperature  $T_2$  increased as the slider-valve opened gradually. The temperature  $T_1$  gets higher than  $T_2$  as the slider-valve failed to close. The oil temperature  $T_3$  at the bottom of the heating chamber remained at ambient temperature throughout the experimental time which was not the case in Figures 7 (~40–50 °C) indicating that there was negligible

thermal conduction from the top hot oil to the bottom due to the continuous oil flow.

The experiment that produced Figure 8 was performed about 3 months after producing Figure 7. When the expansion system is left un-used for a much longer period of time, air enters into it via the rubber seals in the pneumatic cylinder leading to a fast expansion and low contraction due to the air-oil mixture. Figure 8 shows that the slider-valve opened at a temperature lower than preset due to the fast expansion since air expands more than oil. Failure of the air-oil mixture to contract led to the failure of the slider-valve to close leading to a steady increase in the charging temperature with time as observed in Figure 8 between the 15<sup>th</sup> and 55<sup>th</sup> minutes before switching off the heater.

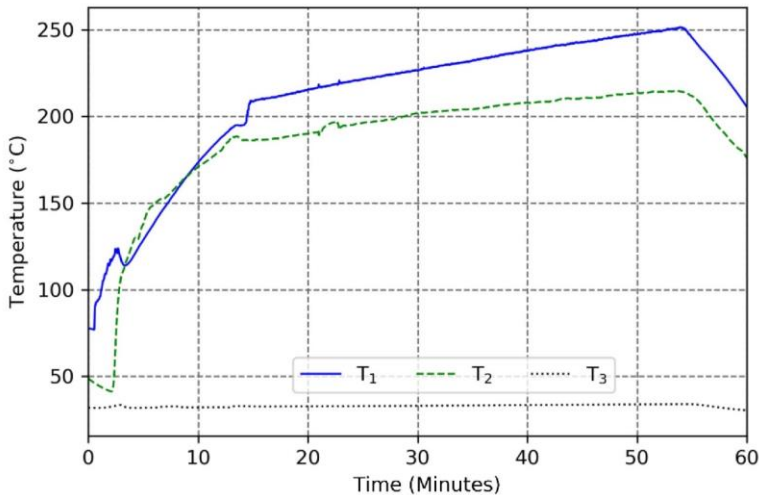


**Figure 8:** Temperature profiles at the top of the heating chamber ( $T_1$ ), at the slider-valve outlet ( $T_2$ ), at the bottom ( $T_3$ ) of the heating chamber when the valve is half-way opened.

After about 15 minutes, the oil temperature  $T_1$  attained a value of 200 °C. When oil stays for longer periods, it at times tries to react with the air and coalesce. This coalescing attempts to block oil flow at low temperature but un-coalesces at high temperature. This possibly explains the kinks in the oil temperature  $T_1$  and  $T_2$  at the 22<sup>nd</sup> minute in Figure 8.

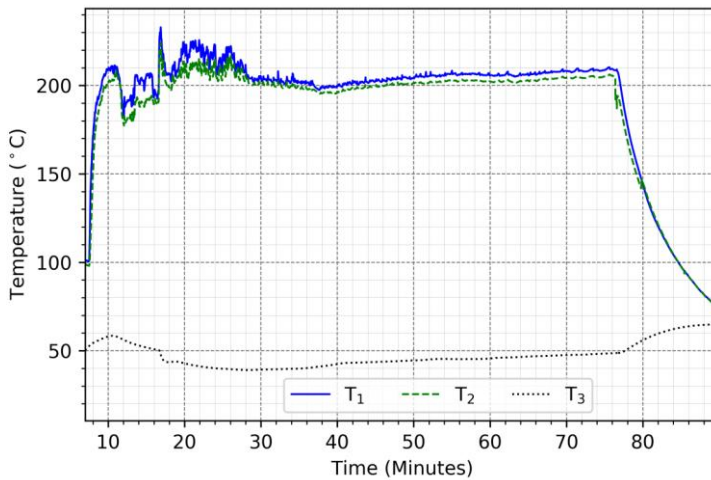
After pumping the air-free oil through the expansion system to remove the air-oil mixture, the cold oil reservoir filled with warm re-used oil and running the experiment at a preset charging temperature of 200 °C with the valve quarter-way opened, we obtained the graphs in Figure 9.

Figure 9 shows that with a partially opened valve, the oil temperatures  $T_1$  and  $T_2$  rose from 100 °C to 213 °C in 8 minutes. The

oil temperatures of  $T_1$  and  $T_2$  were not initial at ambient because of not waiting for the heating chamber to cool to ambient before re-using it, but this does not affect the regulation process at 200 °C according to Equation (2). Having inlet oil to the heating chamber at a higher temperature only reduces on the thermal energy required to attain the preset charging temperature. Within the first 30 minutes, the regulated charging temperature range was  $200 \pm 25$  °C. On leaving the system to stabilize before switching off the heater, the charging temperature range reduced to  $200 \pm 10$  °C. The unexpected larger fluctuations in the first 30 minutes could be attributed to non uniform flow that

usually occurs at the start of any slow fluid flow.

The temperature  $T_3$  at the bottom of heating chamber was at  $\sim 50$  °C as in Figure 7 and varied within a range of 20 °C. At this regulated charging temperature of 200 °C, 0.048 litres of hot oil were collected at the slider-valve in 30 minutes. Therefore, by partially opening the valve, the oscillations observed in Figure 7 were reduced significantly as shown in Figure 9. The heat losses to the ambient we ignored since they do not affect the process of regulating the charging temperature to a nearly constant temperature.



**Figure 9:** Temperature profiles at the top of the heating chamber ( $T_1$ ), at the slider-valve output ( $T_2$ ), at the bottom ( $T_3$ ) of the heating chamber when the valve is quarter-way opened.

**Volume of oil collected**

The volume of hot oil collected in Figures 7 and 9 and the number of slider-valve openings were converted to volume per hour and tabulated in Table 1.

Table 1 shows that the volume of hot oil delivered to the storage tank in one hour reduces whenever the charging temperature increases. This is because more thermal energy is required to heat the oil to higher

temperature since we used a fixed thermal power source. More hot oil can be delivered to the storage tank at a high temperature when the heating power is increased. From Table 1, the mechanical thermostat can deliver about 3.4 litres at 230 °C and 0.096 litres at 200 °C of hot oil in 1 hour to the TES system with oscillating and constant charging temperatures, respectively.

**Table 1:** Summary of the volume of hot oil collected in litres and charging temperatures (T).  $V_{\text{open}}$  is volume of hot oil delivered to the storage tank for each opening of the slider-valve, and  $V_{\text{hour}}$  is the expected volume of hot oil collectable in 1 hour.  $n_{\text{open}}$  is the expected number of slider-valve openings in 1 hour.  $T_{\text{osci}}$  and  $T_{\text{const}}$  represent the oscillating and constant charging temperatures, respectively.

	T °C	$V_{\text{hour}}$ (litres)	$n_{\text{open}}$	$V_{\text{open}}$ (litres)
$T_{\text{osci}}$	116	13.3	8	1.66
	150	11.7	7	1.68
	230	3.4	3	1.13
$T_{\text{const}}$	200	0.096		

The volume of oil delivered to the TES system for each opening of the slider-valve depends on how fast the expansion system responds to temperature changes. It is desired to have fewer slider-valve openings that last for short time periods to ensure minimal thermal losses. The response of the expansion system depends on internal variables of the system that cannot easily be adjusted. These include: the expansion coefficient of the air-free oil and the friction on the rubber-seals in the pneumatic cylinder and on the walls of the slider-slot in the slider-valve. The lower the flow rate at which the hot oil is delivered to the TES system, the more thermal losses to the ambient. This explains the big difference in the volume of hot oil delivered to the TES system at 230 °C in oscillating mode and at 200 °C in the non-oscillating mode in Table 1.

### Solar energy equivalence of the 800 W electric heater

Although the 800 W 220V electric heater was used for heating purposes while testing the developed mechanical thermostat, its equivalent solar energy heating power could be obtained using a solar concentrator or PV system. Uganda receives a direct solar irradiance of 500–700  $\text{Wm}^{-2}$  (Okello et al. 2011). Solar cell efficiencies have reached over 40% and solar thermal systems provide efficiencies in the range 40–80% (Guter et al. 2009, Goswami and Kreith 2017, Hasan et al. 2018, Indira et al. 2020). Taking an average solar thermal conversion efficiency of ~50% for an average solar radiation intensity of ~600  $\text{Wm}^{-2}$ , then an 800 W heating rate would be achieved by a solar concentrator with an area of 2.7  $\text{m}^2$ . Thermal heating could

also be achieved using commercially available PV systems whose efficiency lies in the range 15–20%. Taking an average PV conversion efficiency of ~17.5% for an average solar radiation intensity of ~600  $\text{Wm}^{-2}$ , then an 800 W heating rate would be achieved by a PV system using solar panels with an area of 7.6  $\text{m}^2$ . This shows that in spite of using an electric heater for a thermostat meant for solar systems, it can also be operated using a PV system or solar concentrator.

### Coefficient of volume expansion

The oil level in the heating chamber measured from the bottom reduced from 0.5 m at a temperature of 200 °C to 0.42 m at 25 °C. Using equations 3 and 4, the coefficient of volume expansion of this oil was estimated to lie in the range  $(9.1 \pm 2.1) \times 10^{-4}$  per °C, which agrees with the manufacturer's value of  $7.6 \times 10^{-4}$  per °C (BPS 2005). All linear measurements were made using either a meter rule with an error of  $1.0 \times 10^{-4}$  m or a Vernier caliper with an error of  $1.0 \times 10^{-5}$  m. The temperature measurements using k-type thermocouples were with an error of 0.5 °C (Tong 2001).

### Estimating the active oil volume in the expansion system

With the assumption that, the change  $\Delta V$  in the volume  $V$  of oil in the expansion system or in the equivalent volume to be equal for any temperature change, then the equivalent volume  $V$  could be estimated. This volume change of  $\Delta V = (12.5 \pm 0.6) \times 10^{-3}$  litres at 200 °C was obtained as the product of the maximum extension at 200 °C in

Figure 6 and the cross-sectional area of the pneumatic cylinder. Using equations 3 and 5, the equivalent volume of  $V = (24.8 \pm 5.7) \times 10^{-3}$  liters was obtained.

### Conclusion

A mechanical thermostat has been developed and demonstrated in charging an oil based TES systems at a fairly constant temperature. The temperature regulation was either in oscillatory mode due to the opening and closing of the slider-valve or in constant temperature mode at a fixed flow rate. The oscillatory nature of the thermostat's charging mechanism was studied at three preset charging temperatures of 116 °C, 150 °C and 230 °C where 13.3, 11.7 and 3.4 litres of hot oil could be delivered to the TES system in 1 hour, respectively. The variations in the charging temperatures were reduced by the partial opening of the valve along the pipe from the cold oil reservoir. An averagely constant charging temperature of  $200 \pm 10$  °C was achieved. The ability of this thermostat to control the charging temperature while charging TES systems using low power sources makes it suitable for harnessing solar energy radiation that is usually intermittent in nature.

The expansion system could be improved such that when it stays unused for some time air does not leak through the rubber-seals reducing its thermal sensitivity in regulating the charging temperatures.

### Declaration of Competing Interest

The authors declare that there is no conflict of interest regarding this work.

### Acknowledgements

The authors are grateful to the Norwegian Agency for Development Cooperation (NORAD) for financially supporting this research through the Energy and Petroleum (EnPe 5) project and the SIDA (the Swedish International Development Agency) through International Science Programme (ISP), Uppsala University) for additional support for the dissemination of results through workshops.

### References

- BPS S 2005 *Data Sheet for Shell thermia B*. pds. Retrieved on 27-02-2021 from [www.2kwy.net/pds/pdf/Shell Thermia Oil B PDS v01.pdf](http://www.2kwy.net/pds/pdf/Shell_Thermia_Oil_B_PDS_v01.pdf)
- Brown GO 2002 *The history of the Darcy-Weisbach equation for pipe flow resistance*.
- Crapiste GH, Bredvan MIV and Carelli AA 1999 Oxidation of sunflower oil during storage. *JAOCs J. Am. Oil Chem. Soc.*
- Cuce E and Cuce PM 2013 A comprehensive review on solar cookers. *Appl. Energy* 102: 1399-1421.
- Fernandez-Seara J, Uhi FJ and Sieres J 2007 Experimental analysis of a domestic electric hot water storage tank. Part II: dynamic mode of operation. *Appl. Therm. Eng.* 27(1): 137-144.
- Gallagher A 2011 A solar fryer. *Solar Energy*.
- Goswami DY and Kreith F 2017 *Global Energy Systems*. In *Energy Conversion* (pp. 1-30). CRC Press.
- Guter W, Schöne J, Philipps SP, Steiner M, Siefer G, Wekkeli A, Welser E, Oliva E, Bett AW and Dimroth F 2009 Current-matched triple-junction solar cell reaching 41.1% conversion efficiency under concentrated sunlight. *Appl. Phys. Lett.* 94(22): 223504.
- Haller MY, Cruickshank CA, Streicher W, Harrison SJ, Andersen E and Furbo S 2009 Methods to determine stratification efficiency of thermal energy storage processes—review and theoretical comparison. *Solar Energy*. 83(10): 1847-1860.
- Hand DJ 2011 *Measurements and their Uncertainties: A Practical Guide to Modern Error Analysis*. (Wiley Online Library).
- Hansen EE and Bogsnes C 2018 Self-regulating oil based heat storage. Trondheim.
- Hasan A, Sarwar J and Shah AH 2018 Concentrated photovoltaic: A review of thermal aspects, challenges and opportunities. *Renew. Sustain. Energy Rev.* 94: 835-852.
- Herrmann U and Kearney DW 2002 Survey

- of thermal energy storage for parabolic trough power plants. *J. Sol. Energy Eng* 124(2): 145-152.
- Indira SS, Vaithilingam CA, Chong KK, Saidur R, Faizal M, Abubakar S and Paiman S 2020 A review on various configurations of hybrid concentrator photovoltaic and thermoelectric generator system. *Solar Energy* 201: 122-148.
- Kajumba PK, Okello D, Nyeinga K and Nydal OJ 2020 Experimental investigation of a cooking unit integrated with thermal energy storage system. *J. Energy Storage* 32: 101949.
- Kilian CT 2001 *Modern control technology: components and systems*. Delmar Thomson Learning.
- Lugolole R, Mawire A, Lentswe K, Okello D and Nyeinga K 2018 Thermal performance comparison of three sensible heat thermal energy storage systems during charging cycles. *Sustain. Energy Technol. Assess.* 30: 37-51.
- Kitutu KMG and Diisi J 2014 State of the Environment Report for Uganda. *Kampala: National Environment Management Authority*.
- Mawire A, McPherson M and Van den Heetkamp RRJ 2010 Discharging simulations of a thermal energy storage (TES) system for an indirect solar cooker. *Solar Energy Mater. Solar cell.* 94: 1100-1106.
- Mawire A, Phori A and Taole S 2014 Performance comparison of thermal energy storage oils for solar cookers during charging. *Appl. Therm. Eng.* 73:1323-1331.
- Okello D, Mubiru J and Banda E 2011 Availability of direct solar radiation in Uganda. *30th ISES Bienn. Sol. World Congr.* 3554-3563.
- Okello D, Nydal OJ, Nyeinga K and Banda EJK 2016 Experimental investigation on heat extraction from a rock bed heat storage system for high temperature applications. *J. Energy in South. Afr.*
- Okello D, Omony R, Nyeinga K and Chaciga J 2022 Performance Analysis of Thermal Energy Storage System Integrated with a Cooking Unit. *Energies* 15(23): 9092.
- Schwarzer K and da Silva MEV 2008 Characterisation and design methods of solar cookers. *Solar Energy* 82(2): 157-163.
- Sharp M and Loehrke R 1979 Stratified thermal storage in residential solar energy applications. *J. Energy.* 3(2): 106-113.
- Sjogren OS and Steen AB 2018 *Mechanical temperature control of oil based heat storage* NTNU. <http://hdl.handle.net/11250/2561538>
- Tong A 2001 Improving the accuracy of temperature measurements. *Sensor Review* 21(3): 193-198.